© 2017. Published by The Company of Biologists Ltd | Journal of Experimental Biology (2017) 220, 1852-1863 doi:10.1242/jeb.156265

RESEARCH ARTICLE

Formation and function of intracardiac valve cells in the *Drosophila* heart

Kay Lammers[1,*], Bettina Abeln[1,*], Mirko Hüsken[1,*], Christine Lehmacher[1], Olympia Ekaterini Psathaki[2], Esther Alcorta[3], Heiko Meyer[1] and Achim Paululat[1,‡]

ABSTRACT

Drosophila harbours a simple tubular heart that ensures haemolymph circulation within the body. The heart is built by a few different cell types, including cardiomyocytes that define the luminal heart channel and ostia cells that constitute openings in the heart wall allowing haemolymph to enter the heart chamber. Regulation of flow directionality within a tube, such as blood flow in arteries or insect haemolymph within the heart lumen, requires a dedicated gate, valve or flap-like structure that prevents backflow of fluids. In the *Drosophila* heart, intracardiac valves provide this directionality of haemolymph streaming, with one valve being present in larvae and three valves in the adult fly. Each valve is built by two specialised cardiomyocytes that exhibit a unique histology. We found that the capacity to open and close the heart lumen relies on a unique myofibrillar setting as well as on the presence of large membranous vesicles. These vesicles are of endocytic origin and probably represent unique organelles of valve cells. Moreover, we characterised the working mode of the cells in real time. Valve cells exhibit a highly flexible shape and, during each heartbeat, oscillating shape changes result in closing and opening of the heart channel. Finally, we identified a set of novel valve cell markers useful for future in-depth analyses of cell differentiation in wild-type and mutant animals.

KEY WORDS: Cardiac valves, Cardiogenesis, *Drosophila melanogaster*, Endocytosis

INTRODUCTION

Directionality of blood and lymph flow in vertebrates is regulated by cardiac valves, veins and the vessels of the lymphatic system. The histology of valves differs in adaptation to various pressures and flow rates present in tubular systems. In mammals, the valves that separate the heart chambers consist of a core of connective tissue with collagen and elastin as major constituents whereas venous valves are largely cellular flaps, which are lined with a thin matrix (Armstrong and Bischoff, 2004). Valves passively regulate unidirectional flow when the leaflets of the valve flip to the centre of the vessel and thereby close the luminal space. Several classes of diseases are connected to the dysfunction of valves. Stenosis of cardiac tissue caused by rigidification of the connective tissue prevents valves from closing the lumen completely. Lymphoedema patients suffer from a lymphatic dysfunction resulting in an accumulation of interstitial fluid, which can be caused by abnormal lymphatic valve morphology, e.g. in distichiasis patients in which mutations in the *Foxc2* gene may be causative of the disease (Fang et al., 2000). Besides *Foxc2*, several factors crucial to valve morphogenesis have been identified in human or mouse models in recent years. These include ephrin-B2, Integrin α9 and VEGFR3 signalling components (Bazigou et al., 2011).

The complexity of the circulatory system in vertebrates together with the identification of conserved genes and a functional analogy prompted us to ask whether *Drosophila* can serve as a model to understand basic mechanisms of valve morphogenesis, as well as molecular pathways involved in valve differentiation. Directionality of haemolymph flow within the *Drosophila* larval heart tube is regulated by two means: (i) a directional contraction wave running along the heart tube, and (ii) an intracardiac valve cell that separates the posterior heart chamber from the aorta portion (Lehmacher et al., 2012; Miller, 1950; Molina and Cripps, 2001; Rizki, 1978; Sellin et al., 2006; Wu and Sato, 2008; Zeitouni et al., 2007; present study). Experimental data on how the valves act and on the extent to which they contribute to the control of flow properties within the heart are not yet available. Moreover, specification and differentiation of valve cells have also not been analysed in detail – except for work by Zeitouni and colleagues, who showed that differentiation of the three intracardiac valves present in the adult heart depends on platelet-derived growth factor (PDGF) signalling (Zeitouni et al., 2007). Recent data showed that the transcriptional adapter protein Pygopus, a component of the Wnt signalling pathway, plays a role in differentiation and orientation of the myofibrils in valve cells (Tang et al., 2014). Beside that, little is known about the respective developmental processes.

In the present study, we investigated how intracardiac valve cells work and how they may contribute to the regulation of blood flow directionality in *Drosophila melanogaster*. We found that the valve cells, as a consequence of the contractile forces of the cardiac tube, change their shape synchronously to the heartbeat to effectively close and open the intersection between the heart chamber and the aorta region. Furthermore, we established a data-based model in which the orientation of myofibrils within valve cells is crucial to the periodic switch between a roundish and an elongated shape of the cells. The respective switch is probably essential to proper valve cell performance. In addition, we characterised expression of a *toll*-GFP enhancer line. We show that the enhancer mediates strong reporter gene activity in the intracardiac valves of third-instar larvae, pupae and adults. Finally, utilising a combination of transmission electron microscopy (TEM) analyses and immunohistochemical studies, we characterised the differentiation of the larval valve cells for the first time. We found that large membranous vesicles of endocytic origin, probably unique organelles of valve cells, account for the

[1]University of Osnabrück, Department of Zoology and Developmental Biology, Barbarastraße 11, Osnabrueck 49076, Germany. [2]University of Osnabrück, Biology, EM unit, Barbarastraße 11, Osnabrueck 49076, Germany. [3]Departamento de Biología Funcional, Facultad de Medicina, Universidad de Oviedo, C/Julián Clavería s/n, Oviedo 33.006, Spain.
*These authors contributed equally to this work

‡Author for correspondence (paululat@biologie.uni-osnabrueck)

A.P., 0000-0002-8845-6859

Received 13 January 2017; Accepted 26 February 2017

Journal of Experimental Biology

Journal of Experimental Biology (2017) 220, 1852-1863 doi:10.1242/jeb.156265

characteristic shape of the cells and likely represent the structural basis of their functionality.

MATERIALS AND METHODS

Drosophila strains

Strain w^{1118} was used as a wild type (WT). The *toll*-GFP line (*tl*-GFP) was provided by Robert Schulz (Wang et al., 2005). Gal4 drivers were *hand*C-Gal4 (Hallier et al., 2015; Paululat and Heinisch, 2012; Sellin et al., 2006) and *tin*$^{\Delta}$C-Gal4, provided by Manfred Frasch (Zaffran et al., 2006). All RNAi lines were obtained from the Vienna *Drosophila* Resource Center (VDRC) (Vienna, Austria) (Dietzl et al., 2007). Viking::GFP and UAS-mCD8GFP were obtained from the Bloomington *Drosophila* Stock Center (Bloomington, IN, USA). GFP trap lines (Morin et al., 2001) were provided by the *Drosophila* Genomics and Genetic Resources centre (Kyoto, Japan). The collection of *rab*-Gal4 reporter lines was provided by Robin Hiesinger (Chan et al., 2011).

Immunohistochemistry and TEM

Primary antibodies used were anti-βPS-Integrin [1:3, CF.6G11, supernatant, Developmental Studies Hybridoma Bank (DSHB), Iowa City, IA, USA] and anti-α-Spectrin (1:25, 3A9, supernatant, DSHB). Rabbit anti-GFP (1:1000) was obtained from Abcam (ab6556; Cambridge, UK). Secondary antibodies (Dianova, Hamburg, Germany) were used 1:100 for Cy2-conjugated and 1:200 for Cy3-conjugated antibodies. TRITC-conjugated Phalloidin (Fluka, Sigma-Aldrich, Hamburg, Germany) was used 1:100.

Preparation of semi-thin sections and TEM was performed as described (Albrecht et al., 2011, 2006; Lehmacher et al., 2012, 2009; Tögel et al., 2008).

Animal preparation and image analysis

For bright-field live recordings of valve cells, wandering third-instar larvae were pinned onto Sylgard 184 silicone elastomer plates filled with temperate artificial haemolymph and dissected from the ventral side. After removing viscera and allowing specimens to recover for 10 min, the Sylgard plate was placed on the focusing stage of an upright microscope (Leica DMLB). Heartbeat was recorded with a high-speed video camera with up to 200 frames s^{-1}. Animals that failed to reestablish a regular heartbeat were excluded from analyses. All recordings were made at 22°C to ensure constant conditions for all specimens. Intact non-dissected larvae were glued onto a Sylgard plate with Tissue-Tek® (Sakura) with dorsal side upwards. Artificial haemolymph contains 108 mmol l^{-1} NaCl, 5 mmol l^{-1} KCl, 2 mmol l^{-1} $CaCl_2$, 8 mmol l^{-1} MgCl, 1 mmol l^{-1} NaH_2PO_4, 4 mmol l^{-1} $NaHCO_3$ and 5 mmol l^{-1} Hepes, pH 7.1; prior to use, the buffer was supplemented with sucrose (final concentration 10 mmol l^{-1}) and trehalose (final concentration 10 mmol l^{-1}) (Vogler and Ocorr, 2009). Recordings were captured with a Leica Fluotar (×5, ×10 or ×20) and a Basler piA-640 camera controlled by FireCapture® software (Torsten Edelmann). Recordings were further processed with VirtualDub® (Avery Lee) or with ImageJ (Rasband, 1997-2016). Heart parameters were analysed using SOHA (Semi-Automated Optical Heartbeat Analysis) software (Fink et al., 2009; Ocorr et al., 2014).

Particle injection

Red-coloured monodisperse spheric polystyrene particles with a diameter of 5.2 µm (microParticles GmbH, Berlin, Germany) were dissolved in artificial haemolymph (approximately 1.2×10^3 particles μl^{-1}). A small amount (20 µl) of particle stock solution was pipetted into the posterior half of a semi-intact larva or injected into the posterior body region of an immobilised intact larva or pupa using an Eppendorf microinjector (Femtojet®), a Narishige micro-manipulator and hand-made glass capillaries.

RESULTS

The lumen of the *Drosophila* heart is established by two rows of contralateral-situated cardiomyocytes connected by a dorsal and a ventral adhesion zone (Medioni et al., 2008). In the larva, one pair of cardiomyocytes, which is the 34th pair of cells counted from the anterior, builds the intracardiac valve that partitions the heart tube into an anterior aorta and a posterior heart chamber (Lehmacher et al., 2012; Medioni et al., 2009; Rotstein and Paululat, 2016). During metamorphosis, two additional valves differentiate, resulting in three intracardiac valves in total that subdivide the adult heart into four chambers. The valves in the adult fly are formed by the 22nd, the 28th and the 34th pair of cardiomyocytes (Lehmacher et al., 2012; Rotstein and Paululat, 2016; Tang et al., 2014; Zeitouni et al., 2007).

Intracardiac valve cells – mode of operation

Imaging of valve cells in dissected larvae is technically feasible with bright-field or differential interference contrast (DIC) illumination without the need for additional contrast enhancement. In this study, valve cells were identified based on their position within the heart tube and their unique shape and histology (Fig. 1; Movie 1; and paragraphs below). For each animal we captured several individual recordings, and all recordings were further processed to deduce relevant heartbeat parameters, such as valve cell motility, diastolic and systolic luminal diameters, diastolic and systolic period, or haemolymph streaming velocity.

A typical complete contraction cycle of the heart takes 2.88± 0.08 Hz (corresponds to a heart cycle of ∼347 ms) on average under the conditions used (Fig. 1). This is in line with previous measurements that range between 2.4 Hz and 4.5 Hz (Alex et al., 2015; Gu and Singh, 1995; Sanyal et al., 2006; Sénatore et al., 2010; Sláma and Farkaš, 2005). Several parameters influence heartbeat rate, i.e. temperature (Andersen et al., 2015; Ray and Dowse, 2005), composition of the artificial haemolymph (Zhu et al., 2016) and age (Sláma and Farkaš, 2005; Wessells and Bodmer, 2007).

In the present analysis, we focused on the dynamic activity of the valve cells. First, we aimed to elucidate how the valve cells contribute to closing the heart lumen during each heart contraction cycle. Our analyses of slow-motion recordings revealed that the two valve cells periodically occupy the entire luminal space by changing their shape, thereby closing the heart lumen (Fig. 1A4 and A5). The maximal luminal distance between the opposing valve cells is 77 µm during diastole whereas the heart lumen is completely closed during systole [Fig. 1A1 and B (blue lines)]. The luminal heart diameter posterior to the position of the valve cells varies between approximately 145 µm (diastole) and 72 µm (systole) during a single beating cycle of the heart of a selected individual [Fig. 1A1 and B (red lines)]. A frame-by-frame analysis of the recordings revealed that the closed state persists for approximately 173 ms on average (contact time) in the specimen used to illustrate valve cell behaviour in Fig. 1. This is about one-third of the time of a complete heartbeat cycle. To demonstrate that this value reflects the normal behaviour of valve cells we analysed heart rate and valve cell contact time in several individuals. Although we found minor variations, the mean valve cell contact time always spans one-third of the total time required to complete one heartbeat cycle (Fig. 1C).

Journal of Experimental Biology (2017) 220, 1852-1863 doi:10.1242/jeb.156265

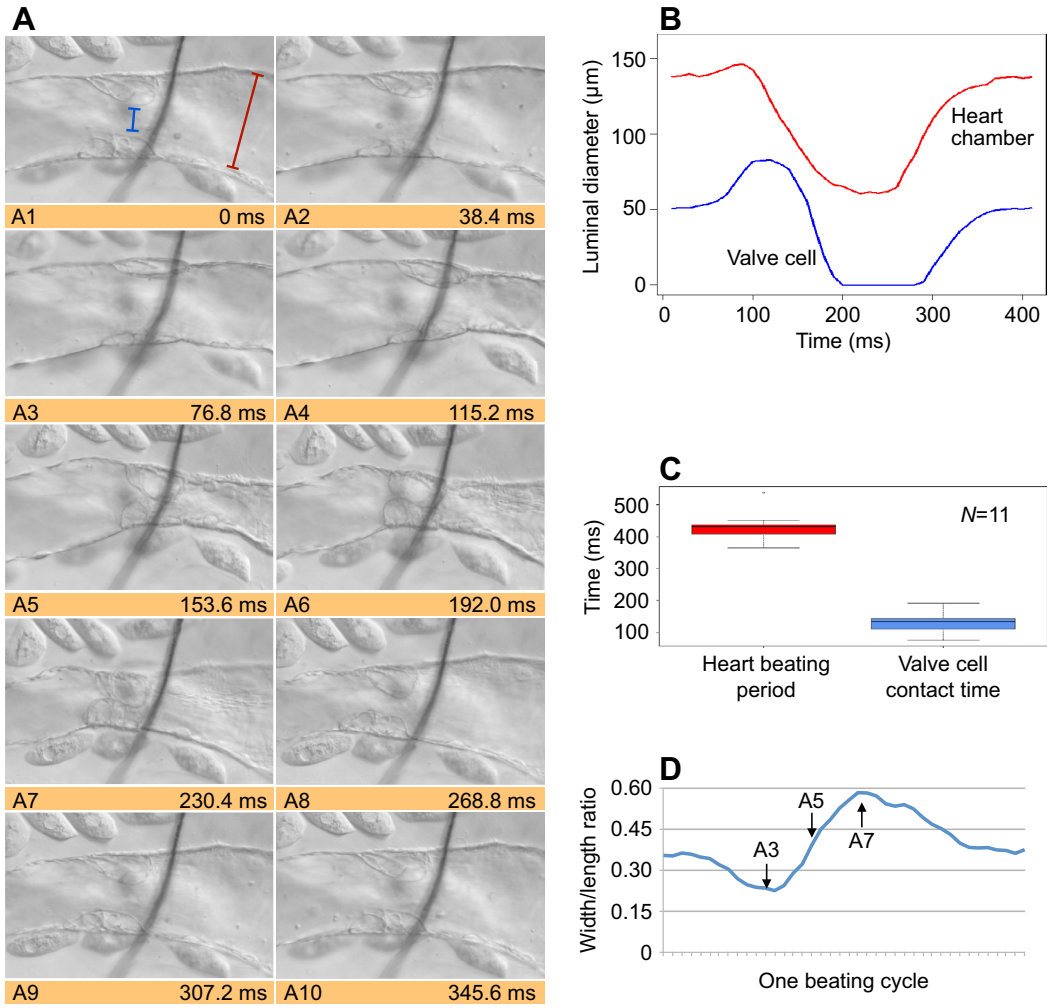

Fig. 1. Video-microscopy analysis of *Drosophila* intracardiac valve motility in semi-intact third-instar larvae. (A) Movement and cell shape change of the intracardiac valve cells was monitored in dissected semi-intact third-instar larvae. Shown are selected single frames from a recording captured at 200 frames s^{-1} (Movie 1). A1–A10 represent, in total, one heartbeat period subdivided into 10 intervals. For example, A3 shows the two valve cells at the maximum luminal distance whereas A6 shows the two valve cells when closing the heart lumen. The black line running across the valve cells is a tracheal branch that runs above the heart and connects the two major dorsal trunks. (B) Several recordings, including the one from which pictures A1–A10 were taken, were used to measure the luminal distance between valve cells (illustrated by a blue line in A1) and between cardiomyocytes constituting the heart chamber (illustrated by a red line in A1). One contraction cycle is shown. Posterior to the valve cells, the luminal diameter oscillates between ~70 µm (systole) and ~150 µm (diastole). Luminal distance between the valve cells oscillates between zero (contact phase, diastole) and ~80 µm (systole). (C) The heartbeat period and valve cell contact time measured in 11 individual animals to illustrate individual variability. On average, the valve cell contact time is one-third of a heartbeat period. The box-and-whisker diagram shows the upper and lower quartiles (first and third quartiles) of the data set, and the median (second quartile) is indicated as a horizontal line inside the box. Vertical lines (whiskers) represent the interquartile range (maximum 1.5 interquartile range), and the outliers are plotted as individual points. (D) As shown in A, the shape of the valve cells oscillates between a roundish shape (e.g. A7) and an elongated spindle-like shape (e.g. A3) during the heartbeat. This is exemplarily illustrated by plotting the width/length ratio of a single selected valve cell against time.

Haemolymph flow in semi-intact third-instar larvae

To assess the relevance of the valve cells to fluid streaming inside the heart, we tracked the movement of particles that were added into the open body cavity of a dissected semi-intact larva (Fig. 2; Movies 2A, 2B, 2C and 4). The particles we used display a high contrast, which allows precise and fast video-based tracking approaches at high frame rates. Thus, we utilised particle injection to study the haemolymph flow inside the heart tube in detail. In this context, the streaming properties alongside the valves of semi-intact specimens were of particular interest.

Evaluation of several recordings substantiated that haemolymph (particles) enters the heart tube via the three pairs of ostia located in the posterior heart chamber. Video analysis further confirmed that during the diastolic filling phase the heart chamber acts as a suction pump. Particles in the outer vicinity of the ostia accelerate during entry into the heart chamber (Fig. 2; Movie 2A). During late diastolic phase, particles move inside the heart chamber but do not pass the valve. Indeed, valve cells are in close contact and thus seal the luminal diameter during this phase. At the beginning of the systolic phase, the valve opens and haemolymph (particles) streams towards anterior (Movie 2B). Streaming velocity is highest within the aorta during the systolic phase. At the end of the systolic phase, haemolymph streaming slows down and the characteristic movement of particles close to the valve indicates turbulent flow in this part of the heart tube (Movie 2B).

Measuring the velocity of the particles within the aorta region revealed that during systole, particles stream inside the heart tube at

Journal of Experimental Biology (2017) 220, 1852-1863 doi:10.1242/jeb.156265

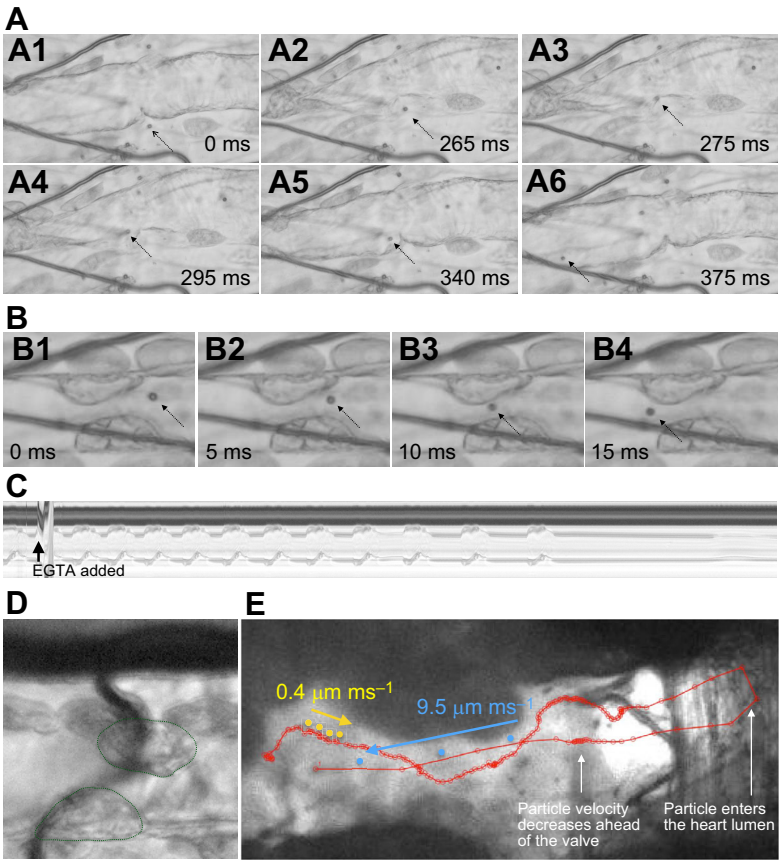

Fig. 2. Injection of coloured polystyrene particles to visualise flow directionality and streaming behaviour in the heart tube. (A) Entry of particles into the heart via ostia was monitored in dissected semi-intact third-instar larvae. A1–A6 represent selected single frames from a recording captured at 200 frames s^{-1} (Movie 2A). This shows that the 5.2 µm polystyrene particles easily enter the heart via the ostial opening present in the heart proper. (B) Illustrates how fast particles pass the valve cells. B1–B4 represent selected single frames from a recording captured at 200 frames s^{-1} (Movie 2B). (C) M-mode trace from a 15 s recording shows heart wall movements in a semi-intact dissected third-instar larva treated with EGTA. Note that the heartbeat slows down and finally stops when treated with EGTA. (D) The valve cells (labelled with a dotted green line) from an animal in which the heartbeat was stopped by EGTA application. The valve cells display a semi-roundish shape. (E) Tracking of an injected particle during a 4 s period taken from a longer recording. An intact white prepupa, glued to a microscopic glass, was injected without dissection. Direction of particle movement is indicated by arrows (yellow, outside of the heart; blue, inside the heart tube). Time interval between each reading point is 20 ms. Note that particles move slower outside the heart lumen (yellow dots, 0.4 µm ms^{-1}, measured for nine particles) and they accelerate in the vicinity of the ostia. Inside the heart proper, particles move towards the anterior and become slower near the valve cells. When the valve opens during the contraction cycle, particles move rapidly into the aorta (blue dots, 9.5 µm ms^{-1}, measured for 14 particles). In addition, the recording illustrates that haemolymph flow is unidirectional and valve cells prevent, in the context of an intact animal, backflow.

approximately 10 µm ms^{-1} (Fig. 2), associated with a Reynolds number (*Re*) of approximately 0.5, indicating that laminar flow conditions are prevalent within the heart tube (velocity ∼0.01 m s^{-1}; density of artificial haemolymph ∼1000 kg m^{-3}; luminal diameter ∼0.15 mm; dynamic viscosity ∼0.001 Pa s^{-1}). It is important to note that we measured only systolic movements in dissected semi-intact third-instar larvae. The reason for this restriction is the fact that during diastole we observed backflow of particles from the aorta into the posterior heart chamber, which we consider artificial and caused by the preparation procedure (see Movie 2C). Visualising haemolymph streaming in intact specimens showed that in larvae and prepupae haemolymph streaming is unidirectional (Choma et al., 2011; Drechsler et al., 2013). This indicates that unidirectional haemolymph flow inside the heart tube is affected by the dissection procedure, presumably due to an impaired connection of the heart tube to the alary muscles.

Haemolymph flow in intact pupae

Particle injection into intact living insects has recently been successfully used to analyse parameters of haemolymph circulation in *Anopheles* (Chintapalli and Hillyer, 2016; League et al., 2015). We now performed such experiments in intact *Drosophila*. It should be noted that image quality dramatically decreased due to limitations caused by the continual darkening of the cuticle (pupa) and the massive line-of-sight obstruction caused by tissues located next to and around the heart tube. Nevertheless, we were able to capture a number of recordings with sufficient quality for further data processing. As a result, we found that the particles behave similarly and exhibit comparable velocities after both injection into intact specimens and application onto dissected animals (Fig. 2E; Movie 4), with one important exception. In contrast to the situation in dissected semi-intact specimens, haemolymph flow in the heart tube of intact animals is clearly unidirectional. This result demonstrates, as expected, that proper heart function requires a closed system, providing high-pressure/low-pressure time windows for efficient heart chamber refilling and pumping phases. Again, we estimated the Reynolds numbers for particles outside of the heart tube and particles that move inside the heart. Due to the limited image quality, we were not able to distinguish clearly between heart chamber, aorta and valve position. Nevertheless, the *Re* is between 0.5 and 10, indicating laminar flow properties within the intact insect body cavity and the heart tube. For a more detailed analysis, it will be necessary to increase image quality, to determine viscosity, and to measure the density of the haemolymph more precisely – issues that will be addressed in future investigations.

Shape dynamics of intracardiac valve cells

During a regular heartbeat, the intracardiac valve cells oscillate between two morphologically distinct states (Fig. 1A1–A10; Movie 1) that determine whether the passage between the heart chamber and the aorta is closed or open. In the open state, each valve cell displays an elongated, flattened shape (Fig. 1A3). With ongoing heart cycle, the valve cells change their shape and become roundish or pear-shaped (Fig. 1A4–A6) and the luminal distance between the valve cells decreases, finally causing a complete closure of the luminal diameter (Fig. 1B) and preventing backflow of haemolymph from the aorta into the heart chamber. We monitored the shape change of valve cells as a function of the relationship between width and length of the cells during heartbeat (Fig. 1D). As a result, we found that valve cells undergo an oscillating deformation process in which the width/length ratio

Journal of Experimental Biology (2017) 220, 1852-1863 doi:10.1242/jeb.156265

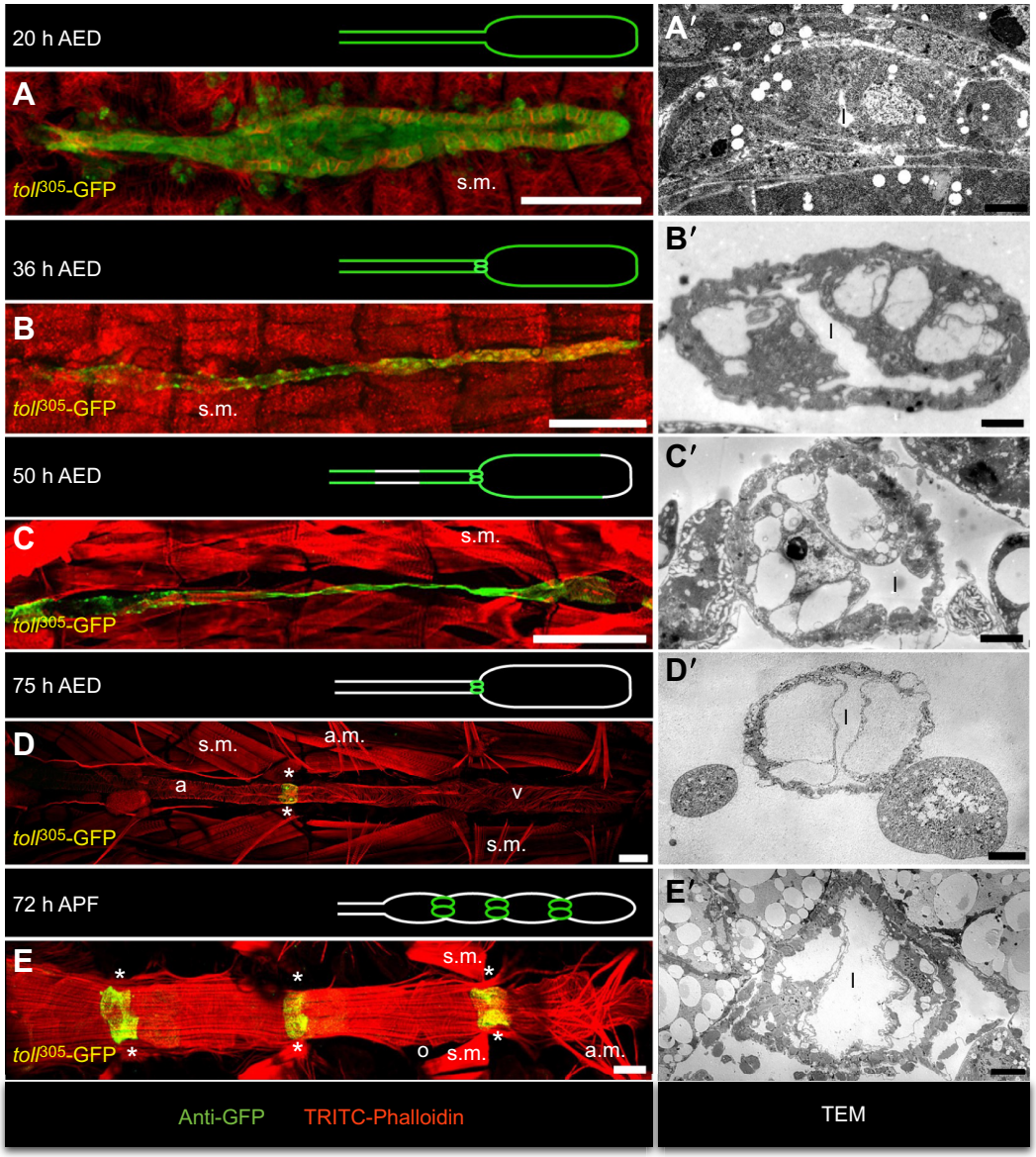

Fig. 3. *toll*-GFP expression in the heart and differentiation of intracardiac valve cells. (A–E) Pictures show the dorsal vessel of a stage 16 embryo (A), larvae (B–D) and an imago (E) stained for GFP (*toll*-GFP, green channel) and Phalloidin (red channel). The broad expression of the *toll*-GFP reporter in all cardiomyocytes of the embryo (A) and the first-instar larvae (B) vanishes in the second-instar larvae (C) and concentrates in the intracardiac valve cells in the third-instar larvae (D, asterisks) and the adult (E, asterisks). A′–E′ show electron micrographs of cross-sectioned valve cells of specimens with the same age. At the ultrastructural level, the embryonic valve cells (A′) are indistinguishable from adjacent cardiomyocytes, compared with Lehmacher et al. (2012). In the first-instar larvae (B′), intracellular vesicles arise and occupy most of the cell volume at the end of the third-instar larval stage (D′). Valve cells in the adult (E′) display the same histology with respect to the valvosomes. In E′, a cross section through the posterior valve cells is shown. a, aorta; AED, after egg laying; a.m., alary muscle; APF, after puparium formation; l, heart lumen; o, ostia; s.m., somatic muscle; v, ventricle. Scale bars: 50 µm (A–E), 2.5 µm (A′–C′) and 10 µm (D′,E′).

changes by a factor of two during one cardiac cycle. The nucleus, which is a less deformable compartment of the cell, dictates to some extent the shape of the cell in the closed state (e.g. Fig. 6). Because of the unique histology of the valve cells (see below), we consider two mechanisms that may allow the extensive shape changes: (i) the cell changes its shape upon contraction but keeps its volume constant, or (ii) the cells oscillate between a compressed and a relaxed state with variable volumes. To address these possibilities, we conducted immunostainings on third-instar larval hearts. We argue that the concomitant fixation arrests the valve cells either in the elongated, in the roundish or in an intermediate state. Subsequent stainings with anti-Spectrin antibodies and evaluation of randomly picked images were then used to reconstruct the valve cells in 3D and to measure, by approximation, the volume of the cells. The corresponding results indicate that valve cell volume remains constant during contraction, suggesting that cell compression plays only a minor role, if any.

Identification of molecular markers to study differentiation of valve cells

The availability of molecular markers, antibodies or valve cell-specific reporter constructs represents a prerequisite for future studies on the differentiation and function of the intracardiac valves. To identify such markers, we screened a GFP protein trap-in collection available at the Kyoto DGGR Stock Center for larval heart and intracardiac valve cell expression. Furthermore, we

Journal of Experimental Biology (2017) 220, 1852-1863 doi:10.1242/jeb.156265

included publicly available transgenic GFP-reporter lines with expression in embryonic cardiomyocytes in our screening, arguing that GFP expression is presumably maintained in all or in a subset of heart cells throughout development. Finally, we analysed the expression of *rab* genes. We did this because our ultrastructural analysis of valve cells (see paragraphs below) revealed that the unique morphology of this cell type is established predominantly by huge vesicular structures within the cells. Since Rab proteins are key regulators of vesicle trafficking and turnover, participation of Rab family members in the formation of these vesicles appears likely.

Interestingly, our screening of publicly available GFP-reporter lines identified only one transgenic *Drosophila* line that exhibited very high GFP expression in larval and adult intracardiac valve cells and virtually no expression in other heart cells (Fig. 3). This particular line has been generated and described earlier by the Schulz laboratory (Wang et al., 2005). It expresses GFP under the control of a 305 bp *toll* enhancer element in all cardiomyocytes of the embryonic dorsal vessel. We found that the broad embryonic *toll*-GFP expression diminishes during transition from the first- to second-instar larval stage (Fig. 3B,C) and is later upregulated in the valve cells of third-instar larval hearts (Fig. 3D). At this developmental stage, the two cells constituting the larval valve are the only cardiomyocytes with remarkable GFP expression. Valve cell-specific GFP expression in this line persists during metamorphosis, and in the adult fly all three pairs of valve cells are strongly labelled (Fig. 3E). Thus, *toll*^{305}-GFP (*toll*-GFP herein) is an excellent marker to visualise the differentiation of valve cells in the larval and adult heart of living or fixed animals. Furthermore, this reporter line is highly beneficial in order to identify the position of the valve cells in histological studies, such as TEM analyses.

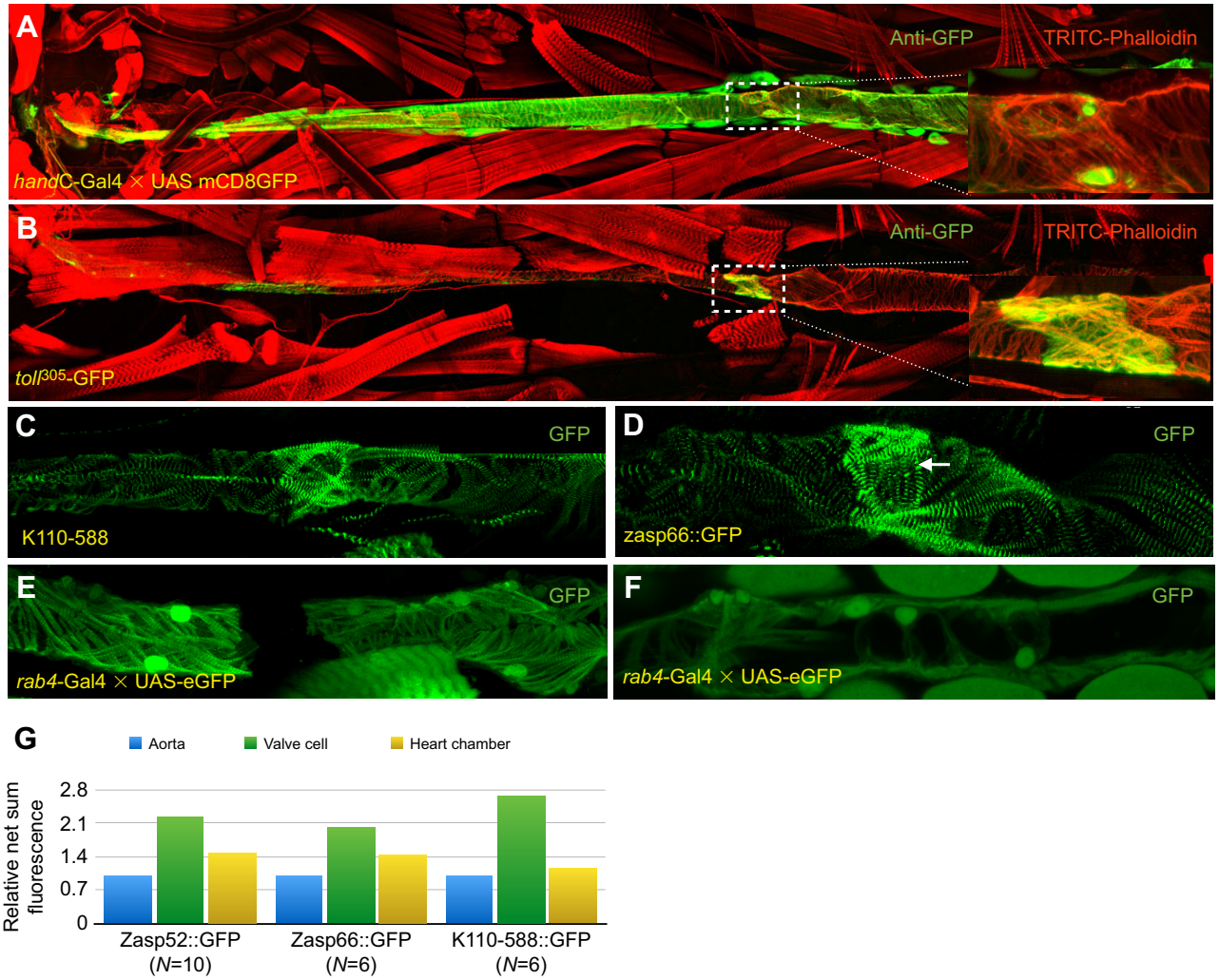

Fig. 4. Markers for intracardiac valve cells in third-instar larvae. (A) The cardiac valve cells of a third-instar larval heart show a higher density of actin–myosin filament network than the adjacent cardiomyocytes. To label all heart cells, *hand*-driven mCD8-GFP (green channel) was used. TRITC-coupled Phalloidin (red channel) was used to label actin filaments. (B) A 305 bp genomic fragment from the *toll* gene drives expression of the GFP reporter in the heart cells with very high peak expression in the valve cells (green channel). TRITC-Phalloidin was used to stain actin filaments (red channel). (C) The GFP protein trap line K110-588 (Morin et al., 2001) enables visualisation of the sarcomeres in cardiomyocytes and the somatic muscles. The valve cells display a higher number of sarcomeres than the adjacent cardiomyocytes. (D) The same result was obtained when analysing the GFP protein trap line K110-740 (Morin et al., 2001) in which the GFP is inserted into the *zasp66* gene. (E,F) GFP expression driven by *rab*-Gal4 enhancer lines. The *rab4* enhancer drives GFP strongly in all cardiomyocytes with the exception of the valve cells (E) whereas the *rab5* enhancer is active in all cardiomyocytes (F). (G) In total, 22 stacks with valve cells labelled for Zasp52::GFP (*N*=10), Zasp66::GFP (*N*=6) and K110-588 (*N*=6) were processed with ImageJ using the 'sum slices' plug-in to calculate the net sum fluorescence intensity of all myofibres present in a valve cell (green), in a cardiomyocyte of the aorta (blue) and the heart chamber region (yellow). Density of myofibres is highest in valve cells.

Journal of Experimental Biology (2017) 220, 1852-1863 doi:10.1242/jeb.156265

Among the GFP protein trap lines (Morin et al., 2001), we identified several lines displaying GFP expression in sarcomeres of third-instar larval cardiomyocytes (Fig. 4C,D). Strongest expression in intracardiac valve cells was apparent in lines in which GFP is trapped to Zasp52 (K110-621, not shown), CG14669 (K110-588, Fig. 4C) and Zasp66 (K110-740, Fig. 4D). These lines were subsequently applied to characterise density and orientation of myofibres in valve cells.

We also analysed 27 lines in which the *gal4* gene was trapped to the open reading frame of one of the *Drosophila rab* encoding genes (Chan et al., 2011). Each line was crossed to a UAS-eGFP effector line and analysed for GFP expression within the hearts of third-instar larvae. We found several lines lacking any detectable cardiac-specific GFP fluorescence (*rab 3*, *9*, *10*, *14*, *19*, *26*, *27*, *30*, *32*, *40*, *X4*, *X5*, *X6*) whereas another set of lines displayed GFP expression in all cardiomyocytes, including valve cells [*rab 1*, *2*, *5* (Fig. 4F), *6*, *7*, *8*, *11*, *23*, *35*, *X1*]. Of note, certain *rab*-Gal4 lines exhibited a strongly reduced, presumably absent, level of GFP expression in valve cells, compared with the adjacent cardiomyocytes [*rab 4* (Fig. 4E), *18* (only some individuals), *21*, *39* (only some individuals)]. The latter group of lines might be useful to express reporter genes or other transgenes in all cardiomyocytes, except for the valve cells.

Valve cells exhibit a unique myofibril architecture

It was described earlier that the intracardiac valves display an intense criss-cross meshwork of sarcomeres (Fig. 4A–D) that distinguishes them from all other cardiomyocytes (Lehmacher et al., 2012; Monier et al., 2005). To substantiate this initial observation, we investigated the orientation and density of myofibres in valve cells systematically using the GFP protein trap lines mentioned above. We used unfixed, dissected third-instar larval hearts from animals expressing Zasp66::GFP, Zasp52::GFP or K110-588::GFP to measure the volume fluorescence intensity of anterior- and posterior-located cardiomyocytes in comparison with valve cells by using the 'sum slices' plug-in of ImageJ. In contrast to the sum fluorescence intensity of cardiomyocytes of the aorta, which was arbitrarily set to 1, the sum fluorescence intensity of valve cells was increased 2.3-fold and the sum fluorescence intensity of cardiomyocytes of the posterior heart chamber was increased 1.4-fold (Fig. 4G). We conclude from these results that the valve cells, compared with other cardiomyocytes, are highly contractile, indicating that myogenic activity represents an important factor enabling the cells to perform the characteristic oscillating shape changes described above (Fig. 1D).

Next, we asked whether myofibres in valve cells display a similar orientation and meshwork structure compared with adjacent cardiomyocytes. Orientation of myofibres in dipteran heart cells is described as circular, which allows contraction of the heart tube and thereby haemolymph transport through the heart lumen (Angioy et al., 1999; Lehmacher et al., 2012; Wasserthal, 1999). However, in valve cells the orientation of myofibres often appeared reticulated. In addition, we found numerous myofibrils that extended from the cell membrane towards the luminal membrane of the valve cell [Fig. 4D (arrow)]. Myofibrils with such an orientation were not found in the adjacent cardiomyocytes. We postulate that the specific architecture of the myofibrillar network accounts for the characteristic contraction dynamics and shape changes valve cells perform during the diastolic and systolic phases of heart contraction.

Based on the observations described above, we speculated that contraction of myofibres, especially those that orientate perpendicular to the *a*–*p*-axis, converts the valve into the open state, which is characterised by an elongated shape of the individual cells (Fig. 1A1–A4). This elongation and the concomitant withdrawal from the luminal space presumably results in a maximum flow rate of haemolymph through the valve. By contrast, relaxation of the valve's myofibres might result in a roundish shape, promoted by the vesicular compartments of the valve cells, and thus closure of the heart lumen. To test this hypothesis, we added the Ca^{2+} chelator EGTA to semi-intact third-instar larvae in order to induce muscle relaxation (Fig. 2C,D). As expected, shortly after EGTA application (arrow in Fig. 2C) the heartbeat stopped. Significantly, adding EGTA also caused the valve cells to adopt a semi-roundish shape (Fig. 2D); thus, muscle tension indeed represents a key factor determining valve cell shape. The result that the heart lumen was not completely closed (Fig. 2D) is presumably due to the fact that the dissection procedure caused an impairment of the functional anatomy, e.g. disconnection of alary muscles and heart tube, which might be relevant to the correct histology and function of valve cells.

Valve cell differentiation starts post-embryonically with the formation of large vesicular compartments

The characteristic histology of the intracardiac valve cells in adult flies was already noticed by Miller (1950), Rizki (1978) and Zeitouni et al. (2007) and led to the description of valve cells as 'spongy' cells. The 'spongy' appearance is caused by large cavities or vesicles that can be visualised with bright-field illumination, immunohistochemistry or TEM (Figs 1, 3 and 5). In this study, we established the timepoint during development at which valve cells start to differentiate and to form their typical histology. Because the total number of cells that build the heart tube is the same in embryos and larvae, and neither cell death nor cell division takes place during this developmental period, valve cell progenitors must already be present in the embryonic heart. The larval valve is built by the 34th pair of cardiomyoblasts and we argue that, in the embryo, this pair of cardiomyoblasts represents the progenitor of the functional valve cells. TEM analyses of stage 16–17 embryos revealed that these prospective valve cells are histologically indistinguishable from adjacent cardiomyocytes at this stage of development (Fig. 3A′). Reference images for cardiomyocytes can be found elsewhere (Lehmacher et al., 2012). The first differences at the ultrastructural level between valve cells and adjacent cardiomyocytes became obvious in late first-instar larvae (about 36 h after egg laying). Some larger and several smaller membranous vesicles, occupying a large portion of the cell's total volume, were abound in the cytoplasm of the two prospective valve cells (Fig. 3B′). Interestingly, such vesicles were only present in valve cells and not in any adjacent cardiomyocytes of this or of later developmental stages. Incipient in second-instar larval stage and lasting until the end of the third-instar larval stage, the valve cells increase in size due to cell growth, and the characteristic vesicles mature into a small number of large vesicles, the valvosomes, which now occupy most of the cell's volume (Fig. 3C′,D′). During metamorphosis, a second and a third pair of valve cells differentiate at defined positions within the heart, resulting in a total of three valves in the adult fly (Fig. 3E) (Lehmacher et al., 2012; Sellin et al., 2006; Tang et al., 2014; Zeitouni et al., 2007). These adult valve cells also harbour the characteristic large vesicles, indicating that the functional anatomy of larval and adult valve cells is, in principle, the same.

Observations from live imaging (Fig. 1; Movies 1, 2A, 2B, 2C and 3), TEM, as well as previous work (Miller, 1950) clearly indicate that the large vesicles, which occupy most of the valve cell volume, represent an important structural element that defines the

Journal of Experimental Biology (2017) 220, 1852-1863 doi:10.1242/jeb.156265

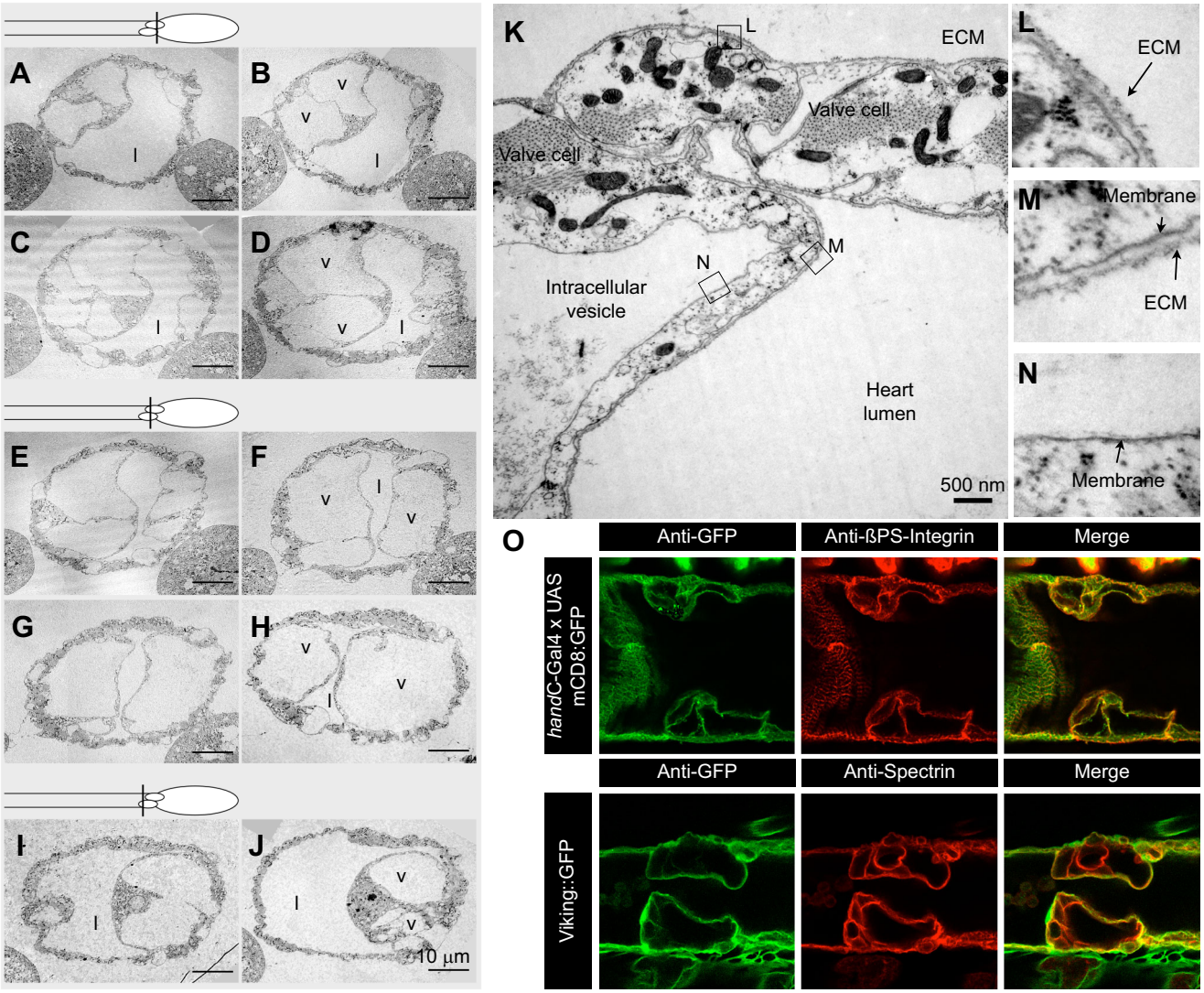

Fig. 5. Ultrastructure of valve cell. (A–J) Selected ultra-thin cross sections taken from a series of 70-nm sections through the valve cells of third-instar larvae of wild type (WT). The three schemes illustrate the corresponding position in the heart, respectively. A is from the posterior and J from the anterior. (K) A cross section through an intracardiac valve cell at high magnification. Shown is the dorsal adhesive zone where the two opposite valve cells meet. ECM is detectable on the cell membrane facing the body cavity (L) and on the cell membrane facing the cardiac lumen (M) but is nearly absent on the inner side of the vesicle membrane (N). (O) Illustrates the membranous nature of the valve's vesicles. The upper row shows anti-GFP (green) and anti-βPS-Integrin (red) staining of valve cells. Note that mCD8::GFP and Integrin label the vesicles. The bottom row shows anti-GFP (green) and anti-Spectrin (red) staining of valve cells. GFP is expressed as a Collagen::GFP fusion protein (Viking::GFP) and is not detectable at the vesicles whereas Spectrin clearly outlines these organelles. l, lumen; v, vesicle.

shape (and probably also the function) of the valve cell. To verify this hypothesis, we analysed the larval valve cells at lower (Fig. 5A–J) and higher (Fig. 5K–N) magnification using ultra-thin serial sections for TEM analysis. Three-dimensional reconstruction of the cells revealed that 50–80% of their volume is occupied by the cavities (Lehmacher et al., 2012, and this study) – a result supporting the assumption that the cavities represent important structural elements. Their membranous nature is verified by two independent approaches. First, we analysed cross sections at higher magnification with TEM (Fig. 5K–N) and found that the intracellular cavities are essentially extracellular matrix (ECM)-free membraneous structures (Fig. 5N). By contrast, the cell membranes, which face the body cavity of the animal or the cardiac lumen, are decorated with electron-dense ECM (Fig. 5L,M). In addition, we stained the valve cells of larvae with antibodies that recognise either Spectrin, a cytoskeletal protein that lines the intracellular side of plasma membranes, or βPS-Integrin, a protein that assembles into membrane-spanning heterodimers (Fig. 5O). For co-staining, we used either mCD8 to label membranes or Viking::GFP, which labels CollagenIV, an ECM protein (Fig. 5O). Anti-βPS-Integrin and anti-Spectrin antibodies both recognised epitopes lining the large cavities inside the valve cells, indicating the membranous nature of these structures (Fig. 5O). This finding is further supported by co-localisation with membrane-associated mCD8-GFP expressed under the control of the cardiac-specific *hand*C-Gal4 driver [Fig. 5O (upper row)] (Paululat and Heinisch, 2012; Sellin et al., 2006). Our results are in agreement with a previous analysis (Lehmacher et al., 2012) that also described the membranous nature of the cavities (Fig. 5K–N). To visualise the presence or absence of ECM proteins at the membranes of the cavities, we used protein traps for Trol/Perlecan (Trol::GFP) or CollagenIV (Viking::GFP, shown herein). We found that the respective matrix proteins are not detectable at the inner surface of the cavities [Fig. 5O (bottom row)], indicating the absence of

Journal of Experimental Biology (2017) 220, 1852-1863 doi:10.1242/jeb.156265

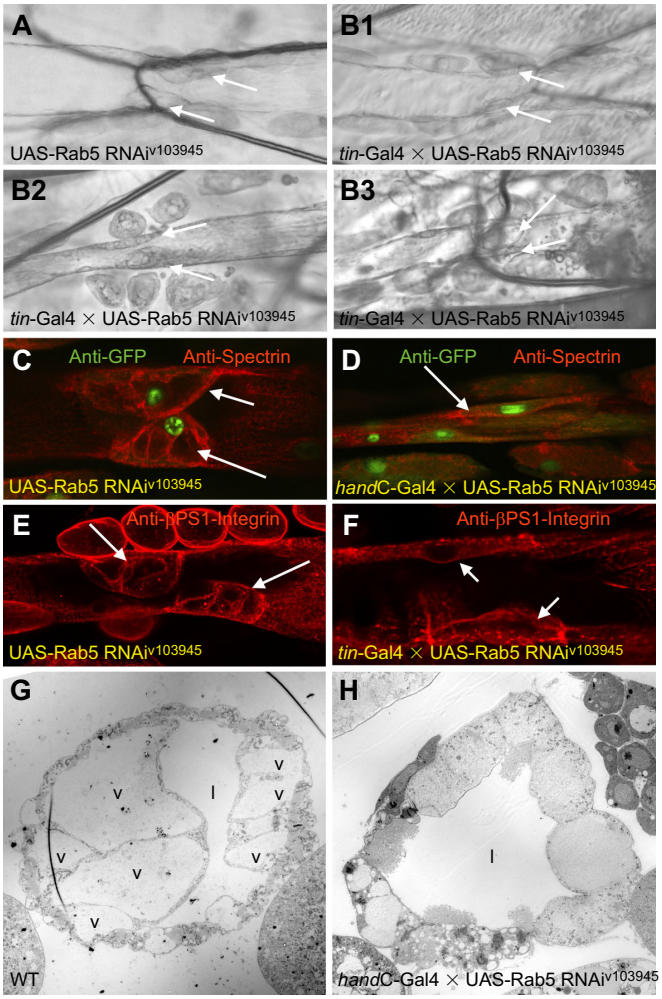

Fig. 6. RNAi-mediated phenotypes in valve cells. (A and B) Selected single frames from recordings captured at 200 frames s^{-1}. (A) Illustrates the valve cells from an animal with the genotype yw; UAS-Rab5 RNAi^{v103945} (control). (B1–B3) Show the valve cells in three different animals with the genotype yw; *tin*-Gal4; UAS-Rab5 RNAi^{v103945}. The valve cells lack their typical histology and overall appearance. (C) The heart of a third-instar larva with the genotype yw; *hand*C-Gal4; *hand*C-GFP, stained for anti-GFP (nuclei of all cardiomyocytes) and anti-Spectrin (outlines the cell membrane) (maximum projection). The typical histology of the valve cells is seen. (D) The heart of a third-instar larva with the genotype yw; *hand*C-Gal4; *hand*C-GFP, UAS-Rab5 RNAi^{v103945}, stained for anti-GFP (nuclei of all cardiomyocytes) and anti-Spectrin (outlines the cell membrane) (maximum projection). Downregulation of Rab5 inhibits valve cell differentiation. The typical histology is not visible. (E) The heart of a third-instar larva with the genotype yw; UAS-Rab5 RNAi^{v103945} (control), stained for anti-βPS1-Integrin (maximum projection). Both valve cells with their characteristic appearance are recognisable. (F) The heart of a third-instar larva with the genotype yw; *tin*-Gal4; UAS-Rab5 RNAi^{v103945}, stained for anti-βPS1-Integrin (maximum projection). Downregulation of Rab5 results in inhibition of valve cell differentiation. Ultra-thin cross sections of valve cells from wild type (WT) (G) and from animals in which Rab5 was downregulated (H) were analysed using transmission electron microscopy (TEM). Mutant valve cells lack the characteristic large membraneous vesicle free of material and display several additional abnormalities. Knockdown specificity was tested using two independent RNAi lines, with the following results: *tin*-Gal4×UAS-RNAi^{v34096} gives rise to 20% of animals with valve cell abnormalities, *tin*-Gal4×UAS-RNAi^{v103945} results in 64% of animals with valve cell abnormalities. (A–F) White arrows point to valve cells. l, lumen; v, vesicle.

ECM material inside the valve cavities. By definition, membranous vesicles within a cell are assigned to certain types of organelles that exert diverse functions in metabolism, trafficking or storage. The large vesicles described herein represent yet unassigned, unique cellular microcompartments. Because of their exclusive appearance in valve cells, we named these vesicles ‘valvosomes’ and suggest the designation for future use.

Downregulation of *rab5* results in valve cells with aberrant vesicle content

The giant vesicles present in valve cells may arise *de novo* as derivatives of the Golgi apparatus (like lysosomes), upon endocytosis (like endosomes), upon membrane invagination (like pinosomes) or as a result of a combination of these processes, including vesicle fusion, which may predominantly account for the increase in size of the valvosomes upon larval development. As a proof-of-principle approach, we inhibited vesicle turnover and endosome maturation in particular by inducing RNAi-mediated downregulation of *rab5* expression. The *rab5* gene is expressed in all cardiomyocytes, including the intracardiac valve cells (Fig. 4). We chose Rab5 as a target because it was shown that inactivation of the protein inhibits a broad range of early endocytic events (Somsel Rodman and Wandinger-Ness, 2000). To ensure knockdown specificity, we analysed two independent *rab5*-RNAi constructs (IR34096, IR103945). Both lines display WT intracardiac valve cells. However, when crossed to a heart-specific Gal4 driver line – here we used *tin*-Gal4 – the third-instar larval offspring displayed severely mis-differentiated valve cells (Fig. 6). Typically, downregulation of *rab5* resulted in smaller valve cells. Yet, the extent of the phenotype was variable and ranged between cells that were only slightly reduced in size to valve cells that were nearly indistinguishable from the adjacent cardiomyocytes (Fig. 6B1–B3, D and F). In addition, while in most cases both valve cells were affected, we also found animals where only one cell was reduced in size. Of note, the reduced size of the valve cells was caused primarily by absence or malformation of the valvosomes (Fig. 6). We are aware of the fact that downregulation of *rab5* may induce a broad range of effects on cell differentiation and cell physiology. Nevertheless, reduction or absence of valvosomes in valve cells as a result of *rab5* knockdown indicates that endocytotic processes are crucial to valve cell differentiation. Characterising these processes in detail will be a major task of future investigations.

DISCUSSION

Fluid flow in biological tubes is a fundamental phenomenon for which a variety of solutions has evolved in animals. In many cases, flow directionality is ensured by the presence of valves or gate-like barriers that prevent backflow. Biological tubes with such barriers include, e.g. renal tubes, lymphatic vessels, the digestive tract and the circulatory system. Valves enhance the efficiency of directional flow and thereby the organ’s overall performance. Despite the simple tube-like architecture of the *Drosophila* heart, numerous studies have demonstrated the suitability of the fly heart to investigate physiology and genetics of cardiogenesis, and cardiac function in general. In contrast to the vertebrate heart, the *Drosophila* cardiac system is not coupled to oxygen transport, and heart failure does not result in immediate death. Nevertheless, flies with certain genetic defects in cardiac development and function suffer from reduced fitness and longevity (e.g. Drechsler et al., 2013; Ocorr et al., 2007). However, specific manipulations of the cardiac ECM may increase longevity (Sessions et al., 2016). Since severe malformations of the heart, or even a complete non-functional heart, do not necessarily result in lethality, consequences of severe heart malformations or heart failure can be examined in living animals. This established *Drosophila* as an ideal model for

Journal of Experimental Biology

Journal of Experimental Biology (2017) 220, 1852-1863 doi:10.1242/jeb.156265

studying heart development and physiology. Herein, we focused on the analysis of the intracardiac valve in *Drosophila*. Although known for a long time, the respective cells have not been studied in detail. We now characterised the histology, presented molecular markers for future in-depth studies, included functional data, and used RNAi-mediated gene knockdown to investigate formation and differentiation of the intracardiac valve cells.

Intracardiac valve cells regulate the directionality of haemolymph flow inside the heart tube

The pumping activity of the tubular heart in insects ensures haemolymph circulation within the open body cavity. The directionality of haemolymph flow is thought to be regulated by distinct anatomical features of the heart tube. One is represented by flap-like cells – the ostia – that constitute the inflow tract, through which the haemolymph enters the heart lumen. A single ostia is built by two flap-like cells. In total, the *Drosophila* heart harbours six (larvae) or 10 (adult) functional ostia that regulate the inflow of haemolymph into the heart proper (Hetz et al., 1999; Iklé et al., 2008; Lehmacher et al., 2012; Molina and Cripps, 2001; Ryan et al., 2005). In larvae, the ostia allow haemolymph to enter the heart during diastole and prevent, due to their flap-like histology, backflow from the heart proper into the body cavity during systole. When haemolymph enters the heart, only the heart proper is filled, indicating that a barrier situated between the heart proper and the anterior aorta ensures efficient refilling. This barrier is constituted by the intracardiac valve, which represents a second anatomical structure preventing backflow and which has been analysed in detail in the present study. The intracardiac valve consists of two histologically unique cells. During each cardiac cycle, the shape of these two intracardiac valve cells oscillates between an elongated and a roundish appearance (Fig. 1A and D). While elongated, the heart lumen stays largely open and allows haemolymph streaming from the heart chamber towards the aorta (Figs 1 and 2). By the end of the systolic phase, the valve cells become roundish and touch each other (Fig. 1A,B). At that time, the transition between the heart chamber and the aorta is closed. The contact time of the two valve cells spans about 1/4–1/3 of a complete cardiac cycle (Fig. 1C). Treatment of hearts of dissected third-instar larvae with EGTA, which induces relaxation of myofibres, causes the valve cells to adopt a semi-roundish shape (Fig. 2C,D). This indicates that valve cells, which exhibit a higher density as well as a special arrangement of myofibres compared with the adjacent cardiomyocytes (Fig. 4), elongate upon contraction and become roundish upon relaxation. This direct interconnection between muscle tension and cell shape is remarkable, because it represents a highly robust and effective means to couple heart contraction with valve opening. While the valve cells are likely to be affected by the same contraction wave as the adjacent cardiomyocytes, the individual arrangements of myofibres result in distinct, yet concerted, responses of the two cell types. The unique histology of the valve cells, which we consider the basis for the highly flexible shape of the cells, is discussed below.

Unidirectionality of haemolymph streaming requires an intact body anatomy. We injected microparticles into the bodies of dissected and intact animals to demonstrate flow properties and valve cell functionality. The speed at which the injected particles move inside the heart lumen is about the same in intact and dissected animals (Fig. 2A,B and E). Calculation of the *Re* indicates that free streaming inside the heart tube follows the rules of laminar flow. Slow streaming velocities are seen in close proximity to the valve cells upon heart lumen closure. Of note, in dissected animals the net flow of haemolymph is quite low due to the fact that haemolymph streams forwards and backwards. This effect is most likely caused by an inefficient filling phase of the heart proper (Figs 1 and 2; Movie 1). However, injection of microparticles into intact animals clearly demonstrated that haemolymph flow is unidirectional (anterograde) (Fig. 2E; Movies 2A, 2B and 2C). Thus, our results demonstrate that an intact anatomy is crucial to an efficient anterograde haemolymph flow inside the heart and therefore to efficient circulation within the insect.

Differentiation of the intracardiac valve

Intracardiac valve cells have been identified due to their unique histology in the larval as well as the adult *Drosophila* heart (Figs 1–3) (Lehmacher et al., 2012; Miller, 1950; Rizki, 1978; Tang et al., 2014; Zeitouni et al., 2007). In third-instar larvae, one intracardiac valve separates the heart into the anterior aorta and the posterior heart chamber (Fig. 3D). This pair of valve cells persists during pupal development and constitutes the third valve of the adult heart. Two additional valves differentiate from the 22nd and the 28th pair of cardiomyocytes, giving rise to a total of three valves subdividing the adult heart into four separate sections (Fig. 3E). In a candidate screening, we identified several molecular markers that allow identification of valve cells in living or fixed specimens. However, only one reporter line, *toll*-GFP, shows a very strong reporter gene expression in the valve cells of third-instar larvae, pupae and adult flies (Fig. 3). This line, which was generated and described previously (Wang et al., 2005), was subsequently used to label valve cells in animals, e.g. for TEM analysis. Several GFP protein trap lines, predominantly obtained from the collection at Kyoto (Morin et al., 2001), helped to elucidate the unique structure of valve cells. For example, Zasp52::GFP and Zasp66::GFP lines mark the sarcomeres in living cells (Fig. 4C,D). Density and orientation of myofibres differ in valve cells compared with adjacent cardiomyocytes. As stated above, we consider especially the orientation of the myofibres essential to the oscillating shape changes of valve cells. Orientation of myofibres perpendicular to the *a–p*-axis of the heart tube most likely results in *a–p* elongation of the valve cells upon contraction. Indeed, applying EGTA to hearts caused relaxation and a semi-roundish (more relaxed) shape of the valve cells (Fig. 2D). We propose a model in which the density and orientation of the myofibres present in the valve cells are crucial to valve cell functionality. Upon contraction, the valve cells convert from a roundish into a flattened shape, which converts the heart lumen from a closed to an open state.

Our TEM analysis (Figs 3 and 5) revealed that valve cell differentiation initiates post-embryonically. Valve cells become histologically distinguishable from the adjacent cardiomyocytes no earlier than in the late 1st-instar larval stage, when the differentiating valve cells start to adopt a unique shape with an expansion towards the heart luminal space (Fig. 3). During second- and third-instar larval development, the valve cells display some characteristic features that turned out to be unique to this cell type: (i) a periodical heartbeat-dependent change between an elongated and a roundish shape, (ii) a more intense myofibre network and a distinct myofibre orientation compared with adjacent cardiomyocytes, and (iii) the appearance of large membranous vesicles that occupy most of the cell volume.

We assume that in fully functional valve cells the large vesicles provide a unique structural element, which allows the cells to easily flatten upon contraction and to effectively expand upon relaxation, thereby opening and closing the luminal space of the heart tube. RNAi-mediated downregulation of *rab5* in valve cells resulted in

cells that failed to adopt the typical roundish shape (Fig. 6B,D,F,H). Besides general cellular defects, *rab5* downregulation affects the formation of the described large vesicles (Fig. 6D,F,H). This result indicates that endosomal maturation plays a major role in valve cell differentiation, which needs to be studied further in the future. Preliminary analyses showed that animals lacking fully differentiated valve cells display problems with sealing the heart lumen during a cardiac cycle. However, there are still no clear data on how this impairment affects streaming properties within the heart. To address this issue, we are currently working on optimising particle injection into living mutant animals, with the aim of reliably visualising haemolymph streaming inside the heart. Several methods have been applied to analyse pumping activity of the heart in adult *Drosophila* (Choma et al., 2010), prepupal *Drosophila* (Drechsler et al., 2013) and adult *Anopheles* (Glenn et al., 2010), but these methods lack the possibility of tracking individual particle movements inside the heart lumen. It will thus be interesting to analyse how mutant valve cells modulate hydrodynamic parameters, such as velocity and directionality of haemolymph flow, *in vivo*.

Drosophila intracardiac valve cells and mammalian endocardial cushion cells

Cardiac valves in *Drosophila* and in the mammalian heart have the same function that is the regulation of flow directionality. This function however is achieved by a different histology: single cells harbouring large intracellular vesicles (valvosomes) that support cell shape changes in the *Drosophila* system, and multicellular valves that originate from valve endothelial cells (VECs) and valve interstitial cells (VICs) that produce matrix-rich cushions in the vertebrate embryo (Wu et al., 2017). Interestingly, VEGF/PDGF signalling plays a role in the formation of the adult intracardiac valves in *Drosophila* and also in endocardial cushion formation and valve remodeling in mammals (Zeitouni et al., 2007). For none of the mammalian valve models the existence of huge intracellular membranous vesicles (valvosomes) was described. Thus, this feature is presumably unique to the simple single cell valve model. Nevertheless, striking similarities between *Drosophila* and mammalian valves are obvious on the molecular level (VEGF/PDGF pathway) and on the functional level (regulating unidirectional flow).

In conclusion, our work describes the function and significance of intracardiac valve cells and provides first insights into the differentiation and histology of these important cells. Thus, it represents a valuable basis for future studies aiming to understand the development and the mode of operation in more detail.

Acknowledgements

We thank Robert A. Schulz for providing fly stocks. We acknowledge K. Etzold and W. Mangerich for their invaluable assistance with TEM analyses and Mechthild Krabusch and Martina Biedermann for technical assistance. Furthermore we thank Sara Timm, Bianca Esch, Franz Kahlich, Kristina Rauf and Martin Schwärzel for additional help.

Competing interests

The authors declare no competing or financial interests.

Author contributions

Conceptualization, A.P., E.A. and H.M.; Methodology, K.L.; Investigation, K.L., B.A., M.H., C.L., O.E.P.; Writing - Original Draft, A.P.; Writing - Review & Editing, A.P. and H.M., Supervision, E.A., H.M. and A.P. Project Administration, A.P.; Funding Acquisition, E.A. and A.P.

Funding

This work was supported by grants from the Deutsche Forschungsgemeinschaft to A.P. (SFB 944), the Deutscher Akademischer Austauschdienst (IPID program) and from the State of Lower-Saxony (ZN2832). B.A. received a fellowship from the State of Lower-Saxony (Lichtenberg-Stipendium). E.A. was supported by grants from the Ministerio de Economía y Competitividad [SAF2013-48759-P] and the Principado de Asturias [GRUPIN14-012].

Supplementary information

Supplementary information available online at
http://jeb.biologists.org/lookup/doi/10.1242/jeb.156265.supplemental

References

Albrecht, S., Wang, S., Holz, A., Bergter, A. and Paululat, A. (2006). The ADAM metalloprotease Kuzbanian is crucial for proper heart formation in *Drosophila melanogaster*. *Mech. Dev.* **123**, 372-387.

Albrecht, S., Altenhein, B. and Paululat, A. (2011). The transmembrane receptor Uncoordinated5 (Unc5) is essential for heart lumen formation in *Drosophila melanogaster*. *Dev. Biol.* **350**, 89-100.

Alex, A., Li, A., Tanzi, R. E. and Zhou, C. (2015). Optogenetic pacing in *Drosophila melanogaster*. *Sci. Adv.* **1**, e1500639.

Andersen, J. L., MacMillan, H. A. and Overgaard, J. (2015). Temperate *Drosophila* preserve cardiac function at low temperature. *J. Insect Physiol.* **77**, 26-32.

Angioy, A. M., Boassa, D. and Dulcis, D. (1999). Functional morphology of the dorsal vessel in the adult fly *Protophormia terraenovae* (Diptera, Calliphoridae). *J. Morphol.* **240**, 15-31.

Armstrong, E. J. and Bischoff, J. (2004). Heart valve development: endothelial cell signaling and differentiation. *Circ. Res.* **95**, 459-470.

Bazigou, E., Lyons, O. T. A., Smith, A., Venn, G. E., Cope, C., Brown, N. A. and Makinen, T. (2011). Genes regulating lymphangiogenesis control venous valve formation and maintenance in mice. *J. Clin. Invest.* **121**, 2984-2992.

Chan, C.-C., Scoggin, S., Wang, D., Cherry, S., Dembo, T., Greenberg, B., Jin, E. J., Kuey, C., Lopez, A., Mehta, S. Q. et al. (2011). Systematic discovery of Rab GTPases with synaptic functions in *Drosophila*. *Curr. Biol.* **21**, 1704-1715.

Chintapalli, R. T. V. and Hillyer, J. F. (2016). Hemolymph circulation in insect flight appendages: physiology of the wing heart and circulatory flow in the wings of the mosquito *Anopheles gambiae*. *J. Exp. Biol.* **219**, 3945-3951.

Choma, M. A., Suter, M. J., Vakoc, B. J., Bouma, B. E. and Tearney, G. J. (2010). Heart wall velocimetry and exogenous contrast-based cardiac flow imaging in *Drosophila melanogaster* using Doppler optical coherence tomography. *J. Biomed. Opt.* **15**, 056020.

Choma, M. A., Suter, M. J., Vakoc, B. J., Bouma, B. E. and Tearney, G. J. (2011). Physiological homology between *Drosophila melanogaster* and vertebrate cardiovascular systems. *Dis. Model. Mech.* **4**, 411-420.

Dietzl, G., Chen, D., Schnorrer, F., Su, K.-C., Barinova, Y., Fellner, M., Gasser, B., Kinsey, K., Oppel, S., Scheiblauer, S. et al. (2007). A genome-wide transgenic RNAi library for conditional gene inactivation in *Drosophila*. *Nature* **448**, 151-156.

Drechsler, M., Schmidt, A. C., Meyer, H. and Paululat, A. (2013). The conserved ADAMTS-like protein lonely heart mediates matrix formation and cardiac tissue integrity. *PLoS Genet.* **9**, e1003616.

Fang, J., Dagenais, S. L., Erickson, R. P., Arlt, M. F., Glynn, M. W., Gorski, J. L., Seaver, L. H. and Glover, T. W. (2000). Mutations in FOXC2 (MFH-1), a forkhead family transcription factor, are responsible for the hereditary lymphedema-distichiasis syndrome. *Am. J. Hum. Genet.* **67**, 1382-1388.

Fink, M., Callol-Massot, C., Chu, A., Ruiz-Lozano, P., Izpisua Belmonte, J. C., Giles, W., Bodmer, R. and Ocorr, K. (2009). A new method for detection and quantification of heartbeat parameters in *Drosophila*, zebrafish, and embryonic mouse hearts. *BioTechniques* **46**, 101-113.

Glenn, J. D., King, J. G. and Hillyer, J. F. (2010). Structural mechanics of the mosquito heart and its function in bidirectional hemolymph transport. *J. Exp. Biol.* **213**, 541-550.

Gu, G.-G. and Singh, S. (1995). Pharmacological analysis of heartbeat in *Drosophila*. *J. Neurobiol.* **28**, 269-280.

Hallier, B., Hoffmann, J., Roeder, T., Tögel, M., Meyer, H. and Paululat, A. (2015). The bHLH transcription factor Hand regulates the expression of genes critical to heart and muscle function in *Drosophila melanogaster*. *PLoS ONE* **10**, e0134204.

Hetz, S. K., Psota, E. and Wasserthal, L. T. (1999). Roles of aorta, ostia and tracheae in heartbeat and respiratory gas exchange in pupae of *Troides rhadamantus* Staudinger 1888 and *Ornithoptera priamus* L. 1758 (Lepidoptera, Papilionidae). *Int. J. Insect Morphol. Embryol.* **28**, 131-144.

Iklé, J., Elwell, J. A., Bryantsev, A. L. and Cripps, R. M. (2008). Cardiac expression of the *Drosophila* Transglutaminase (CG7356) gene is directly controlled by myocyte enhancer factor-2. *Dev. Dyn.* **237**, 2090-2099.

League, G. P., Onuh, O. C. and Hillyer, J. F. (2015). Comparative structural and functional analysis of the larval and adult dorsal vessel and its role in hemolymph circulation in the mosquito *Anopheles gambiae*. *J. Exp. Biol.* **218**, 370-380.

Lehmacher, C., Tögel, M., Pass, G. and Paululat, A. (2009). The *Drosophila* wing hearts consist of syncytial muscle cells that resemble adult somatic muscles. *Arthropod. Struct. Dev.* **38**, 111-123.

Lehmacher, C., Abeln, B. and Paululat, A. (2012). The ultrastructure of *Drosophila* heart cells. *Arthropod. Struct. Dev.* **41**, 459-474.
Medioni, C., Astier, M., Zmojdzian, M., Jagla, K. and Sémériva, M. (2008). Genetic control of cell morphogenesis during *Drosophila melanogaster* cardiac tube formation. *J. Cell Biol.* **182**, 249-261.
Medioni, C., Sénatore, S., Salmand, P.-A., Lalevée, N., Perrin, L. and Sémériva, M. (2009). The fabulous destiny of the *Drosophila* heart. *Curr. Opin. Genet. Dev.* **19**, 518-525.
Miller, A. (1950). The internal anatomy and histology of the imago. In *Biology of Drosophila* (ed. M. Demerec), pp. 420-534. New York: John Wiley & Sons, Inc.
Molina, M. R. and Cripps, R. M. (2001). Ostia, the inflow tracts of the *Drosophila* heart, develop from a genetically distinct subset of cardial cells. *Mech. Dev.* **109**, 51-59.
Monier, B., Astier, M., Sémériva, M. and Perrin, L. (2005). Steroid-dependent modification of Hox function drives myocyte reprogramming in the *Drosophila* heart. *Development* **132**, 5283-5293.
Morin, X., Daneman, R., Zavortink, M. and Chia, W. (2001). A protein trap strategy to detect GFP-tagged proteins expressed from their endogenous loci in *Drosophila*. *Proc. Natl. Acad. Sci. USA* **98**, 15050-15055.
Ocorr, K., Akasaka, T. and Bodmer, R. (2007). Age-related cardiac disease model of *Drosophila*. *Mech. Ageing Dev.* **128**, 112-116.
Ocorr, K., Vogler, G. and Bodmer, R. (2014). Methods to assess *Drosophila* heart development, function and aging. *Methods* **68**, 265-272.
Paululat, A. and Heinisch, J. J. (2012). New yeast/*E. coli*/*Drosophila* triple shuttle vectors for efficient generation of *Drosophila* P element transformation constructs. *Gene* **511**, 300-305.
Rasband, W. S. (1997-2016). *ImageJ*. Bethesda, Maryland, USA: U. S. National Institutes of Health. http://imagej.nih.gov/ij/.
Ray, V. M. and Dowse, H. B. (2005). Mutations in and deletions of the Ca^{2+} channel-encoding gene *cacophony*, which affect courtship song in *Drosophila*, have novel effects on heartbeating. *J. Neurogenet.* **19**, 39-56.
Rizki, T. M. (1978). The circulatory system and associated cells and tissues. In *The Genetics and Biology of Drosophila*, Vol. 2b (ed. M. Ashburner and T. R. F. Wright), pp. 397-452. New York, NY: Academic Press.
Rotstein, B. and Paululat, A. (2016). On the morphology of the *Drosophila* heart. *J. Cardiovas. Dev. Dis.* **3**, 15.
Ryan, K. M., Hoshizaki, D. K. and Cripps, R. M. (2005). Homeotic selector genes control the patterning of seven-up expressing cells in the *Drosophila* dorsal vessel. *Mech. Dev.* **122**, 1023-1033.
Sanyal, S., Jennings, T., Dowse, H. and Ramaswami, M. (2006). Conditional mutations in SERCA, the Sarco-endoplasmic reticulum Ca(2+)-ATPase, alter heart rate and rhythmicity in *Drosophila*. *J. Comp. Physiol. B* **176**, 253-263.
Sellin, J., Albrecht, S., Kölsch, V. and Paululat, A. (2006). Dynamics of heart differentiation, visualized utilizing heart enhancer elements of the *Drosophila melanogaster* bHLH transcription factor Hand. *Gene Expr. Patterns* **6**, 360-375.
Sénatore, S., Rami Reddy, V., Sémériva, M., Perrin, L. and Lalevée, N. (2010). Response to mechanical stress is mediated by the TRPA channel painless in the *Drosophila* heart. *PLoS Genet.* **6**, e1001088.
Sessions, A. O., Kaushik, G., Parker, S., Raedschelders, K., Bodmer, R., Van Eyk, J. E. and Engler, A. J. (2016). Extracellular matrix downregulation in the *Drosophila* heart preserves contractile function and improves lifespan. *Matrix Biol.*, 1-13.
Sláma, K. and Farkaš, R. (2005). Heartbeat patterns during the postembryonic development of *Drosophila melanogaster*. *J. Insect Physiol.* **51**, 489-503.
Somsel Rodman, J. and Wandinger-Ness, A. (2000). Rab GTPases coordinate endocytosis. *J. Cell Sci.* **113**, 183-192.
Tang, M., Yuan, W., Bodmer, R., Wu, X. and Ocorr, K. (2014). The role of Pygopus in the differentiation of intracardiac valves in *Drosophila*. *Genesis* **52**, 19-28.
Tögel, M., Pass, G. and Paululat, A. (2008). The *Drosophila* wing hearts originate from pericardial cells and are essential for wing maturation. *Dev. Biol.* **318**, 29-37.
Vogler, G. and Ocorr, K. (2009). Visualizing the beating heart in *Drosophila*. *J. Vis. Exp.* **28**, 1425.
Wang, J., Tao, Y., Reim, I., Gajewski, K., Frasch, M. and Schulz, R. A. (2005). Expression, regulation, and requirement of the Toll transmembrane protein during dorsal vessel formation in *Drosophila melanogaster*. *Mol. Cell. Biol.* **25**, 4200-4210.
Wasserthal, L. T. (1999). Functional morphology of the heart and of a new cephalic pulsatile organ in the blowfly *Calliphora vicina* (Diptera: Calliphoridae) and their roles in hemolymph transport and tracheal ventilation. *Int. J. Insect Morphol. Embryol.* **28**, 111-129.
Wessells, R. J. and Bodmer, R. (2007). Age-related cardiac deterioration: insights from *Drosophila*. *Front. Biosci.* **12**, 39-48.
Wu, M. and Sato, T. N. (2008). On the mechanics of cardiac function of *Drosophila* embryo. *PLoS ONE* **3**, e4045.
Wu, B., Wang, Y., Xiao, F., Butcher, J. T., Yutzey, K. E. and Zhou, B. (2017). Developmental mechanisms of aortic valve malformation and disease. *Annu. Rev. Physiol.* **79**, 21-41.
Zaffran, S., Reim, I., Qian, L., Lo, P. C., Bodmer, R. and Frasch, M. (2006). Cardioblast-intrinsic Tinman activity controls proper diversification and differentiation of myocardial cells in *Drosophila*. *Development* **133**, 4073-4083.
Zeitouni, B., Sénatore, S., Séverac, D., Aknin, C., Sémériva, M. and Perrin, L. (2007). Signalling pathways involved in adult heart formation revealed by gene expression profiling in *Drosophila*. *PLoS Genet.* **3**, e174.
Zhu, Y. C., Uradu, H., Majeed, Z. R. and Cooper, R. L. (2016). Optogenetic stimulation of *Drosophila* heart rate at different temperatures and Ca^{2+} concentrations. *Physiol. Rep.* **4**, e12695.